Ice flow line maps of three large freshwater calving glaciers in the Southern Patagonian Icefield

Esteban Lannutti[1,2,3], Pablo Marmolejo[2], José Sanchez[2], Ignacio Ortíz[1], María G. Lenzano[1], Silvana Moragues[1,3], Andrés Rivera [4], Paulina Vacaflor[1], Gustavo Pereyra[2], Hugo Morales[2]

[1] Lab. de Geomática Andina (LAGEAN), IANIGLA, CONICET, Argentina - (elannutti, irortiz, mlenzano, smoragues, pvacaflor)@mendoza-conicet.gob.ar
[2] Lab. de Robot Móviles y Manipuladores Autónomos (LARMMA), UTN, FRM, Argentina - pablomarmolejo83@hotmail.com, csanchezz@gmail.com, pereyra28@gmail.com, hugom@frm.utn.edu.ar
[3] Depto. de Geografía, Facultad de Filosofía y Letras, Uncuyo, Argentina
[4] Depto. de Geografía, Universidad de Chile, Chile - arivera@uchile.cl

Keywords: Ice flow lines, Glacier length, Ice dynamics, Viedma glacier, Upsala glacier, Pio XI glacier.

Abstract

The Southern Patagonian Icefield is experiencing rapid retreat and thinning in its calving glaciers. To better understand the dynamics of these changes, we generated ice flow line maps for the Viedma, Upsala, and Pio XI glaciers during 2017–2018. An evenly spaced streamline placement algorithm, integrating topographic and flow curvature criteria, was employed to calculate over 2,700 streamlines per glacier at a 50-meter resolution. The algorithm's performance was assessed by comparing the generated flow lines with manually digitized reference lines, resulting in a mean error, standard deviation, and root mean square error of 57.35, 33.62, and 66.46 meters, respectively. The resulting maps reveal detailed flow structures, highlighting flow lines from accumulation to ablation zones, increased velocities in central areas, tributary flows merging with main channels, and regions of flow convergence and divergence. Additionally, the glaciers' 3D lengths were estimated by identifying the longest ice flow lines, with Pio XI measuring 62.27 km, Viedma 54.49 km, and Upsala 51.24 km. We consider that the methodology used, along with the generated maps, provides excellent visual and analytical tools for identifying glacier areas, lengths, and shapes, defining ice origins and glacier catchment boundaries, and analysing zones of flow convergence and divergence—parameters that are critically important for understanding the dynamics, geometry, and evolution of glaciers in this region.

1. Introduction

Glaciers in mountainous regions have suffered a loss of 123 ± 24 Gt yr^{-1} during 2006-2015 (IPCC, 2022). The Southern Patagonian Icefield (SPI) is a temperate ice mass that spans the territories of southern Chile and Argentina (Figure 1) and constitutes most of the land ice stored in South America (Bown et al., 2019). The SPI extends for about 350 km long between 48°20' and 51°30'S along 73°30'W (Aniya et al., 1997). Over the past decades, its calving glaciers have experienced one of the fastest mass losses in the world (Zemp et al., 2019). Ice dynamics play a major role in the mass change of calving glaciers in this region (Minowa et al., 2023).

The flow patterns of glaciers evolve as their geometry, flow mechanics (i.e., internal deformation and basal sliding), and thermal regime adjust under the influence of internal and external conditions (Ng and Hughes, 2019). The information contained in ice flow velocity and patterns is essential for studying ice dynamics, glacier geometry, evolution, and inventories. It helps to identify glacier areas, lengths, and shapes, define the origin of ice and the limits of glacier catchments, and calculate ice discharge into lakes or the ocean, among many other applications (Le Bris and Paul, 2013; Machguth and Huss, 2014; Mouginot and Rignot, 2015; Yang and Kang, 2022; Nanni et al., 2023). For example, glacier length is one of the central measures representing the geometry of glaciers (Machguth and Huss, 2014). Despite its scientific relevance, glacier length is difficult to define, and determining it manually is a laborious process; therefore, automated computation has gained new relevance (Leclercq et al., 2014; Machguth and Huss, 2014; Zhang et al., 2022).

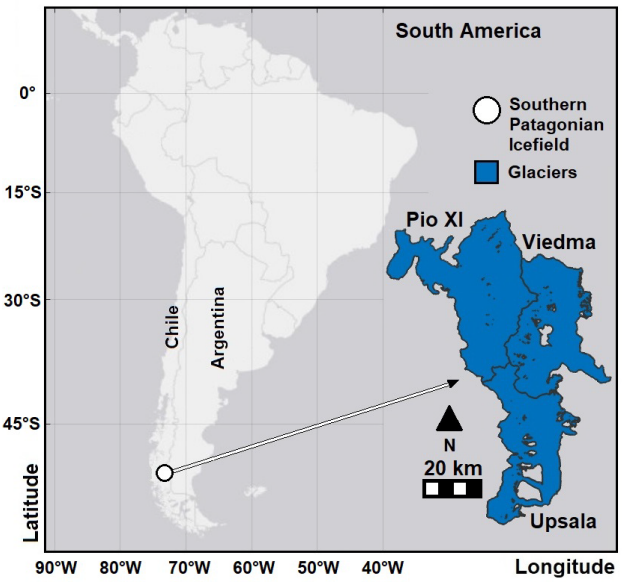

Figure 1. Location of the Southern Patagonian Icefield, and Viedma, Upsala, and Pio XI glaciers.

Flow visualization techniques are prominent tools for studying the flow patterns of glaciers. While various flow visualization methods are available, streamlines are the most widely used. The foundational concepts of streamlines involve defining a flow field as a vector field on a discretized mesh and using integral curves, calculated from seed points through numerical

approximation methods (e.g., the Runge-Kutta method), to visualize particle trajectories within that field (Sane et al., 2020).

Therefore, to contribute to understanding the processes that control ice dynamics and glacier response in the SPI, we developed a streamline algorithm that automatically estimates surface ice flow lines using ice velocity maps and considers topographic and flow curvature conditions to enhance the robustness of the results. Using this algorithm, we extract the surface ice flow lines of Viedma, Upsala and Pio XI—three large freshwater calving glaciers—for the period 2017–2018. Additionally, we compared the algorithm's performance against a set of surface flow lines extracted through manual digitization. Finally, to assess the algorithm's capabilities as a tool for automated glacier geometry computation, it was used to calculate the length of these three glaciers in the SPI.

2. Data and Methods

In our research, we estimated surface flow lines using a streamline algorithm developed by Jobard and Lefer (1997) and Ma (2024). This effective, widely used single-pass method allows for the placement of long, evenly spaced streamlines in a steady-state field. This approach was chosen because even spacing better illustrates the structure of a vector field compared to others that generate streamlines with seed points placed on a regular grid. To further improve the representativeness and coherence of the flow lines corresponding to glacier ice motion, our algorithm restricts the calculation of streamlines based on surface flow curvature and slope criteria. Consider planimetric ice flow with surface velocity u = (u v) ^{T} where u and v are functions of position x = (x y) ^{T} (Ng, Gudmundsson and King, 2018) and x and y are the Utm easting and Utm northing direction. The curvature (χ) and slope (S) are:

$$\chi(x,y) = \frac{\partial \theta_h}{\partial l}, \qquad (1)$$

$$S(x,y,z) = \frac{\partial \theta_v}{\partial l}, \qquad (2)$$

where θ_h, θ_v = horizontal and vertical flow direction vectors
x, y = image coordinates
l = denotes distance along flow
z = elevation derived from Digital Elevation Model

We consider that, physically, the trajectory of ice flow cannot suddenly change direction or flow uphill. Therefore, if abs(χ) and S are less than cc=170°/ 50 m and cs = 7°/ 50 m (cc and cs represent the curvature and slope criteria, respectively) the ice flow at the point (x, y) is accepted. The values of cc and cs were empirically chosen based on the resolution of the input data and the visual coherence and continuity of the generated flow lines.

Using this algorithm, we estimated the ice flow lines of Viedma, Upsala, and Pio XI glaciers with a 50 m spacing. To minimize errors due to the temporal mismatch between the acquisition of input data, we used components that closely aligned with the study period. In this context, the input data for the ice velocity maps (u), Digital Elevation Model, and glacier outlines were sourced from the global dataset 2017-2018 (Millan et al., 2022), TanDEM-X-2011-2015 (TerraSAR-X add-on for Digital Elevation Measurement), and GLIMS-2016 (RGI Consortium, 2017), respectively. The Millan dataset (Millan et al., 2022) uses Sentinel-2/ESA, Landsat-8/USGS, Venμs/CNES-ISA, Pléiades/Airbus D&S, and radar data from Sentinel-1/ESA to calculate ice velocity, achieving an accuracy of about 10 m yr^{-1}.

Then, we evaluated the performance of the algorithm by calculating the mean error (ME), standard deviation (SD), and root mean square error (RMSE) between the automatically generated (x, y) streamlines and the reference flow lines. Given that supraglacial moraines reflect the motion of the ice surface, we manually digitized a series of four moraines per glacier using 10 m Sentinel satellite images (acquisition date: 27 March 2018) to establish reference lines. Evaluating the errors between these reference lines and the calculated streamlines allows us to verify the coherence and accuracy of the algorithm.

Finally, we define glacier length as the length of the longest flow line of a glacier (Nussbaumer et al., 2007; Paul et al., 2009). Therefore, to estimate the three-dimensional length of the three glaciers, we automatically calculated the 3D length (x, y, z) of all streamlines, assuming surface-parallel flow and using the DEM to determine z (up-component). From this, the longest length found for each of the three glaciers was identified, thus determining their lengths.

3. Results

The results of the surface velocity and 2D ice flow lines for the three glaciers under study are shown in Figure 2. The algorithm calculated a total of 2893, 2711, and 3421 streamlines for the Viedma, Upsala, and Pio XI glaciers, respectively. In total, it filtered out more than 2600 trajectories that showed points with reverse and uphill flows, which did not satisfy the curvature and slope criteria. In the figure, the surface flow lines are evenly spaced, effectively illustrating the structure of the vector field. Additionally, important patterns can be observed, such as flow lines extending from the accumulation zones to the ablation zones of the glaciers, higher flow velocities in the central areas, tributary flows converging with the main flow, and various zones of convergence and divergence in the surface ice flow. For more details on specific patterns of surface flow lines, refer to boxes a, b, and c in Figure 2.

Figure 3 shows the manually digitized supraglacial moraines (reference flow lines) alongside the most closely matching streamlines used for algorithm evaluation. Table 1 summarizes the algorithm's performance, presenting the mean errors (MEs), standard deviations (SDs), and root mean square errors (RMSEs) calculated between the reference flow lines and the automatically estimated 2D streamlines (Figure 3). The Upsala and Pio XI glaciers demonstrate similar fits, with the lowest ME and RMSE values. Although the Viedma glacier exhibits slightly higher errors, the algorithm achieves low errors for all three glaciers when considered in relation to the 50 m resolution.

Glacier	ME	SD	RMSE
	m	m	m
Viedma	69.42	33.15	76.89
Upsala	51.13	32.12	60.34
Pio XI	51.51	32.44	60.84
Total	57.35	33.62	66.46

Table 1. ME, SD, and RMSE calculated between the automatically generated streamlines and the reference flow lines, presented for each glacier individually and as an overall average for the three glaciers.

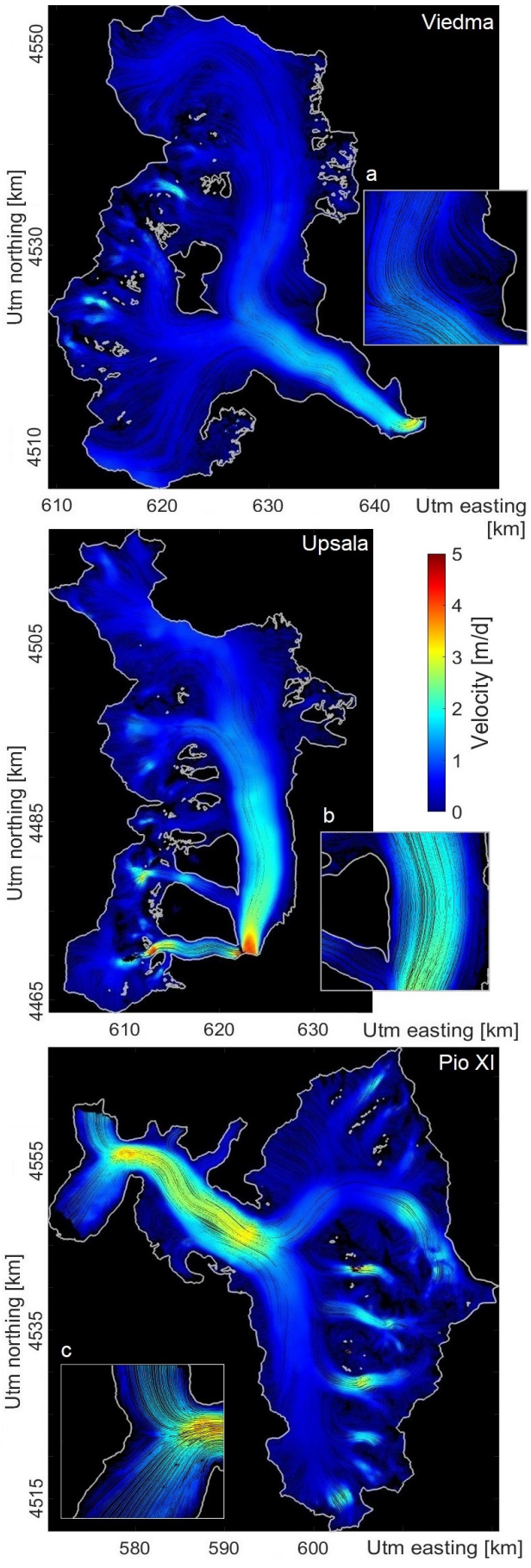

Figure 2. Surface velocity and ice flow lines of the three glaciers, with detailed views provided in boxes a, b, and c.

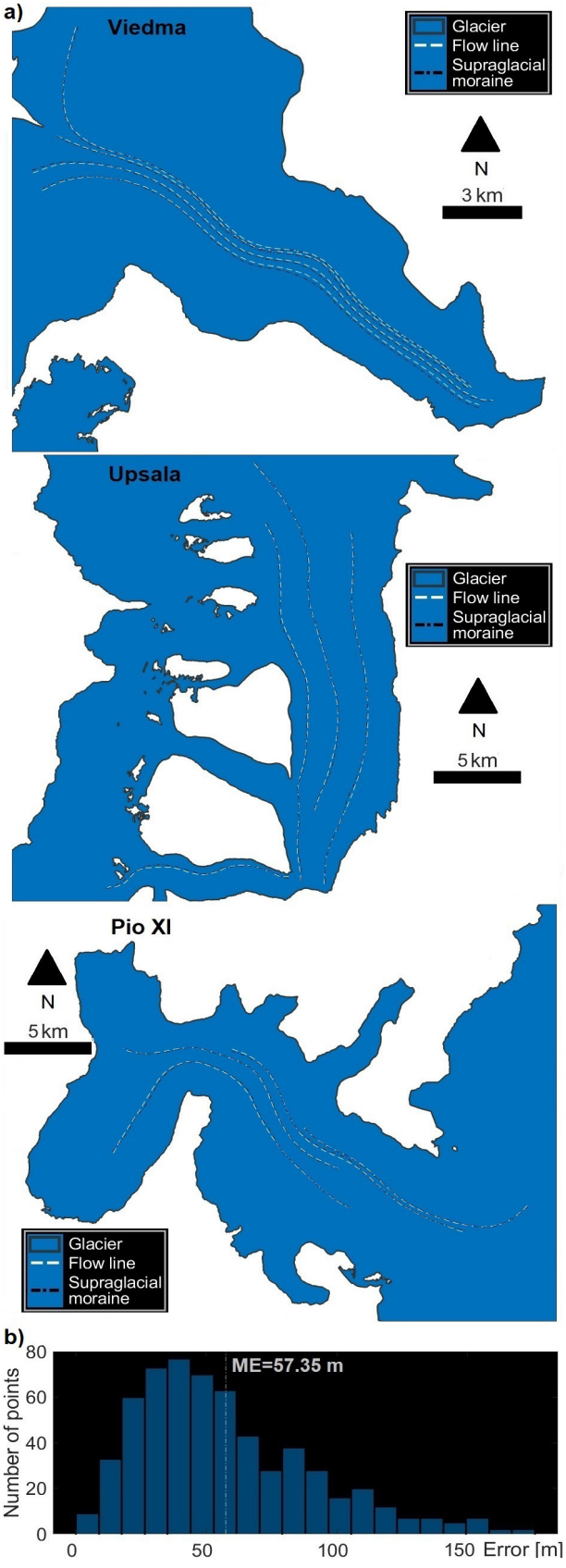

Figure 3. a) Reference flow lines from manually digitized supraglacial moraines (black dash-dotted line) and corresponding streamlines from the algorithm (white dashed line). b) Histogram of total errors for algorithm evaluation, with ME representing the mean error across the three glaciers.

The three-dimensional (x, y, z) glacier lengths calculated for each of the three glaciers are presented in Figure 4.

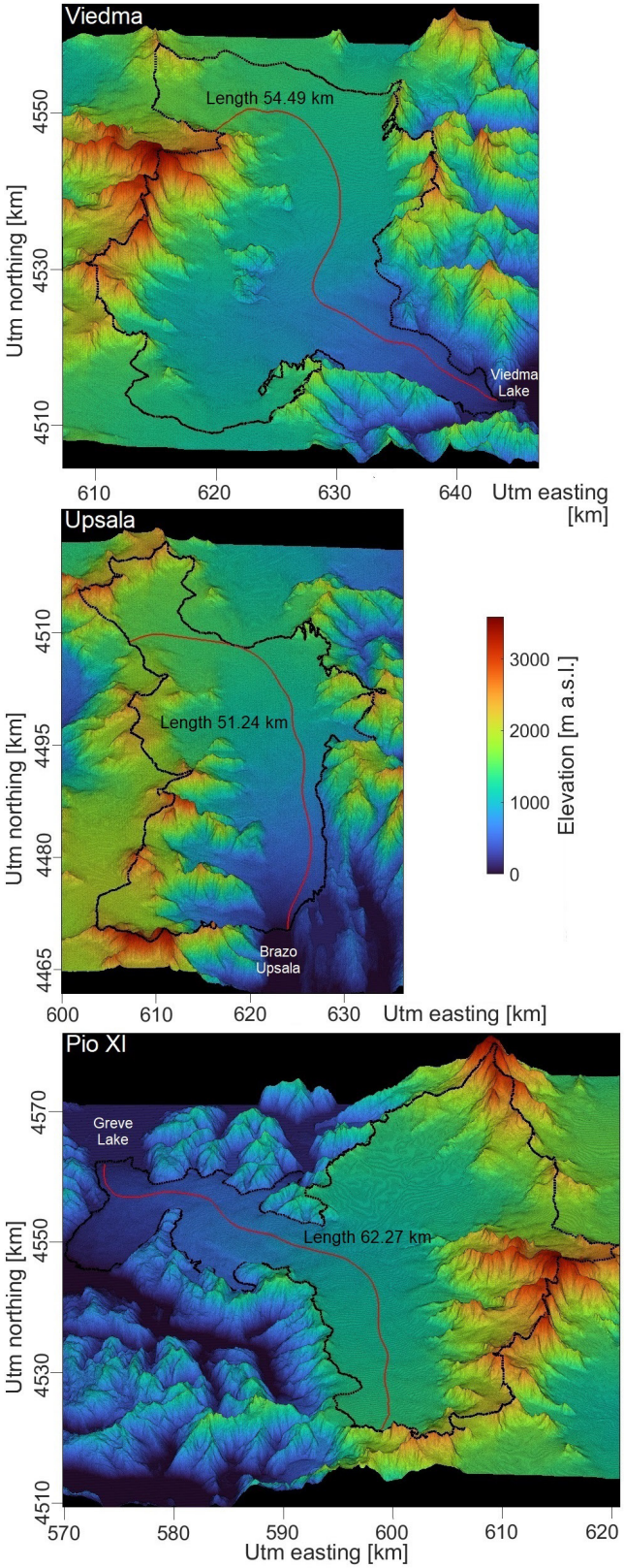

Figure 4. Trajectories of the streamlines (red line) used to estimate the three-dimensional lengths of the Viedma, Upsala, and Pio XI glaciers. The black dashed line corresponds to the glacier outlines.

Pio XI is the glacier with the greatest length (62.27 km), with an elevation difference (Δz) of 1652.0 m between the highest and lowest points of the streamline. The flow line starts in the southernmost accumulation zone of the glacier and ends at the terminus in Greve Lake (Figure 4). Next in length is Viedma glacier, with 54.49 km and a Δz of 2024.9 m. The ice flow begins in the accumulation zone above 2500 m a.s.l. and ends at the northern edge of the glacier front near Viedma Lake. Lastly, Upsala has a length of 51.24 km, with ice flow starting above 1500 m a.s.l. and ending at the front of the Brazo Upsala arm (Figure 4), reaching an elevation difference Δz of 1380 m.

4. Discussion and Conclusion

In the past decade, the availability of high-resolution mapping of surface ice motion in glacial environments has significantly increased. Techniques such as multiple synthetic aperture radar and optical data collection have achieved high spatial-temporal resolutions (e.g., Mouginot et al., 2017; Gardner et al., 2018; Bocchiola et al., 2021; Van Wyk de Vries and Wickert, 2021). The ice flow velocity map derived from multiphase satellite imagery is aligned with the present-day flow direction, which offers key support for the extraction of ice flow patterns (Yang and Kang, 2022). The integration of these velocity maps with the calculation of ice flow patterns provides valuable insights for studying glacier dynamics in Patagonia (e.g., Riggio, 2022; Mouginot and Rignot, 2015).

In our work, we developed detailed maps of ice flow lines derived from surface velocity vector fields of Viedma, Upsala, and Pio XI glaciers in the SPI (Figure 2). While conventional streamline generation algorithms typically rely solely on vector field data, our approach incorporates topographic factors and curvature and slope criteria, which enhance the robustness of the results. As highlighted in Section 3, more than 2600 points produced reverse and uphill flows. The removal of these 2600 trajectories from a total of 8825 significantly improved the final accuracy and representativeness of the calculated ice flow lines. Moreover, when comparing the results with ice motion inferred from manually digitized supraglacial moraines (Figure 3), the algorithm demonstrated good performance, with ME, SD, and RMSE values matching the 50 m resolution of the vector field used (Table 1).

Furthermore, this tool demonstrates great potential for both visualizing and calculating three-dimensional ice flow line. The calculation of three-dimensional lengths—62.27, 54.49, and 51.24 km of Viedma, Upsala, and Pio XI glaciers, respectively (Figure 4)—illustrates the methodology's effectiveness in automatically determining glacier geometry. Another example of its potential is evident in Figure 2, where discrepancies in glacier outlines defined by GLIMS (RGI Consortium, 2017) are apparent. The interruption of streamlines near these glacier outlines suggests errors in their determination. A clear example of this is observed at the northern end of the Upsala glacier, at the boundary with the Viedma glacier. Figure 5 illustrates this case, where a significant portion of the ice flow is directed towards the Viedma basin (indicated by the yellow dashed lines) rather than the Upsala basin. Therefore, according to our methodology, the correct glacier outlines should be located between the yellow and red dashed lines. Aligned with the approach proposed by Mouginot and Rignot (2015), our product combines topography and ice flow trajectories, which better resolve ambiguities in glacier drainage and glacier outlines.

Accordingly, our study enhances the understanding of glacier ice dynamics in the Southern Patagonian Icefield by enabling the

accurate estimation of ice flow lines and the lengths of three of the largest glaciers in one of the world's most significant icefields.

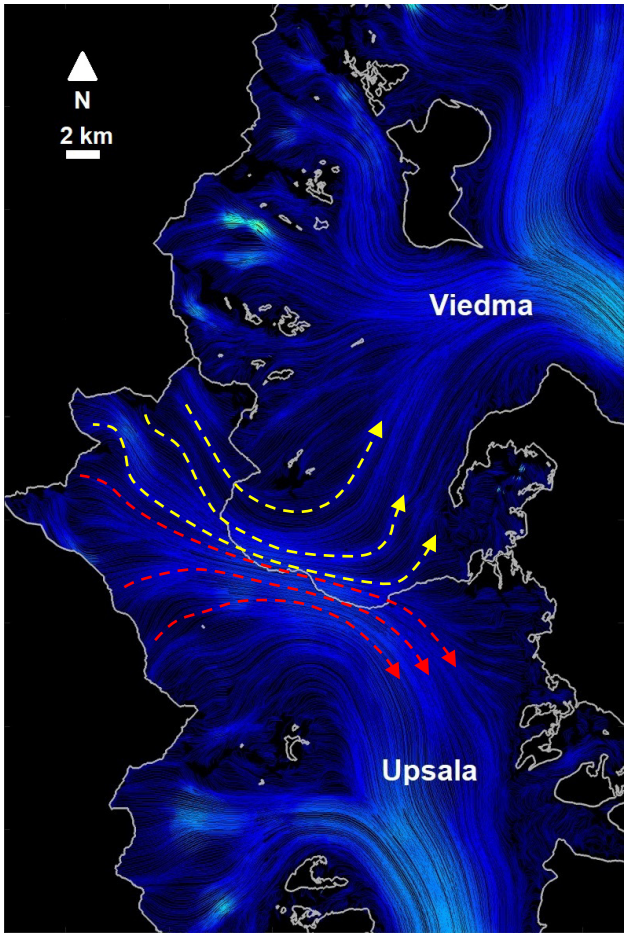

Figure 5. Example of discrepancies in glacier outlines as defined by GLIMS (gray line). The yellow and red dashed lines indicate the streamlines for the Viedma and Upsala glaciers, respectively.

To further explore and develop the potential of this tool, we propose as future work to identify glacier areas and shapes, define the origin of ice and the boundaries of glacier catchments, and then compare these findings with results from other studies conducted in the SPI (e.g., De Angelis, 2014; RGI Consortium, 2017; Zhang et al., 2022). Additionally, we will calculate and analyze zones of flow convergence and divergence based on the generated ice flow line maps.

Acknowledgements

We would like to express our gratitude to the members of the Laboratorio de Geomática Andina, Public Education, Parque Nacional Los Glaciares, Agencia Nacional de Promoción de la Investigación, el Desarrollo Tecnológico y la Innovación, Consejo Nacional de Investigaciones Científicas y Técnicas (IANIGLA-CONICET), Universidad Tecnológica Nacional, Laboratorio LARMMA, Universidad Nacional de Cuyo, and Universidad de Chile for their collaboration and support.

References

Aniya, M., Sato, H., Naruse, R., Skvarca, P., 1997: Recent glacier variations in the Southern Patagonia Icefield, South America. Arctic and Alpine Research, 29(1), 1-12.

Bocchiola, D., Chirico, F., Soncini, A., Azzoni, R. S., Diolaiuti, G. A., 2021: Assessment of recent flow and calving rate of the Perito Moreno Glacier using LANDSAT and SENTINEL2 images. Remote Sensing, 14(1), 52.

Bown, F., Rivera, A., Pętlicki, M., Bravo, C., Oberreuter, J., 2019: Recent ice dynamics and mass balance of Jorge Montt Glacier, Southern Patagonia Icefield. Journal of Glaciology, 65(253), 732-744.
De Angelis, H., 2014: Hypsometry and sensitivity of the mass balance to changes in equilibrium-line altitude: the case of the Southern Patagonia Icefield. Journal of Glaciology, 60(219), 14-28.

Gardner, A. S., Fahnestock, M. A., Agram, P. S., Scambos, T., Nilsson, J., Paolo, F. S., 2018: ITS_LIVE: A new NASA MEaSUReS initiative to track the movement of the world's ice. In AGU Fall Meeting Abstracts (Vol. 2018, pp. C14A-02B).

IPCC, 2022: High mountain areas, The ocean and cryosphere in a changing climate. Cambridge University Press, 131–202 pp., https://doi.org/10.1017/9781009157964.004.

Jobard, B., Lefer, W., 1997: Creating evenly-spaced streamlines of arbitrary density. Visualization in Scientific Computing, 97, 43-55.

Le Bris, R., Paul, F., 2013: An automatic method to create flow lines for determination of glacier length: A pilot study with Alaskan glaciers. Computers & Geosciences, 52, 234-245.

Leclercq, P. W., Oerlemans, J., Basagic, H. J., Bushueva, I., Cook, A. J., Le Bris, R., 2014: A data set of worldwide glacier length fluctuations. The Cryosphere, 8, 659–672, doi:10.5194/tc-8-659-2014.

Ma, K., 2024: Evenly spaced streamlines. (https://github.com/keithfma/evenly_spaced_streamlines), GitHub.

Machguth, H., Huss, M., 2014: The length of the world's glaciers–a new approach for the global calculation of center lines. The Cryosphere, 8(5), 1741-1755.

Millan, R., Mouginot, J., Rabatel, A., Morlighem, M., 2022: Ice velocity and thickness of the world’s glaciers. Nature Geoscience, 15(2), 124-129.

Minowa, M., Schaefer, M., Skvarca, P., 2023: Effects of topography on dynamics and mass loss of lake-terminating glaciers in southern Patagonia. Journal of Glaciology, 1-18.

Mouginot, J., Rignot, E., 2015: Ice motion of the Patagonian icefields of South America: 1984–2014. Geophysical Research Letters, 42(5), 1441-1449.

Mouginot, J., Rignot, E., Scheuchl, B., Millan, R., 2017: Comprehensive annual ice sheet velocity mapping using Landsat-8, Sentinel-1, and RADARSAT-2 data. Remote Sensing, 9, 364.

Nanni, U., Scherler, D., Ayoub, F., Millan, R., Herman, F., Avouac, J. P., 2023: Climatic control on seasonal variations in mountain glacier surface velocity. The Cryosphere, 17(4), 1567-1583.

Ng, F. S., Hughes, A. L., 2019: Reconstructing ice-flow fields from streamlined subglacial bedforms: A kriging approach. Earth Surface Processes and Landforms, 44(4), 861-876.

Ng, F. S., Gudmundsson, G. H., King, E. C., 2018: Differential geometry of ice flow. Frontiers in Earth Science, 6, 161.

Nussbaumer, S. U., Zumbühl, H. J., Steiner, D., 2007: Fluctuations of the Mer de Glace (Mont Blanc area, France) AD 1500–2050: An interdisciplinary approach using new historical data and neural network simulations. Zeitschrift für Gletscherkunde und Glazialgeologie, 40, 1–175.

Paul, F., Barry, R., Cogley, J., Frey, H., Haeberli, W., Ohmura, A., Ommanney, C., Raup, B., Rivera, A., Zemp, M., 2009: Recommendations for the compilation of glacier inventory data from digital sources. Annals of Glaciology, 50, 119–126, doi:10.3189/172756410790595778.

RGI Consortium, 2017: Randolph Glacier Inventory—A dataset of global glacier outlines, Version 6. [Indicate subset used]. Boulder, Colorado, USA. NSIDC: National Snow and Ice Data Center. doi: https://doi.org/10.7265/4m1f-gd79.

Riggio, C., 2022: Bilancio di massa del ghiacciaio Perito Moreno tramite remote sensing e misure radar.

Sane, S., Bujack, R., Garth, C., Childs, H., 2020: A survey of seed placement and streamline selection techniques. In Computer Graphics Forum (Vol. 39, No. 3, pp. 785-809).

Van Wyk de Vries, M., Wickert, A. D., 2021: Glacier Image Velocimetry: An open-source toolbox for easy and rapid calculation of high-resolution glacier velocity fields. The Cryosphere, 15, 2115–2132, https://doi.org/10.5194/tc-15-2115-2021.

Yang, Z., Kang, Z., 2022: Antarctic-scale ice flow lines map generation and basin delineation. Remote Sensing, 14(9), 1958.

Zemp, M., Huss, M., Thibert, E., Eckert, N., McNabb, R., Huber, J., Cogley, J. G., 2019: Global glacier mass changes and their contributions to sea-level rise from 1961 to 2016. Nature, 568(7752), 382-386.

Zhang, D., Zhou, G., Li, W., Zhang, S., Yao, X., Wei, S., 2022: A new global dataset of mountain glacier centerlines and lengths. Earth System Science Data, 14(9), 3889-3913.